CRYSTALLOGRAPHY REPORTS, 2025, Vol. 70, No. 1, pp. 86–92

SURFACE, THIN FILMS

INVESTIGATION OF INHOMOGENEOUS DEFORMATIONS OF CRYSTAL LATTICES DURING DEFORMING CUTTING OF 08X18N10T STEEL SAMPLES WITH PERIODIC SURFACE RELIEF

© 2025 B. E. Vintaikin*, Ya. V. Cherenkov, A. E. Smirnov, and S. G. Vasiliev

Bauman Moscow State Technical University, Moscow, Russia

**e-mail: vintaikb@bmstu.ru*

Received September 04, 2024
Revised November 30, 2024
Accepted December 02, 2024

Abstract. A technique has been developed for obtaining true X-ray diffraction intensity distribution profiles by X-ray diffractometry to detect inhomogeneous surface deformations of a curved surface with periodic relief by separating the effects associated with the influence of this surface on the shape of the diffraction profile. True intensity distribution profiles related only to inhomogeneous surface deformations and crystal block sizes have been obtained, and the parameters and features of the distribution functions of these deformations have been determined. The proposed approach makes it possible to isolate, among other things, the contribution only from a curved surface with a regular relief of the sample to the shape of the intensity distribution profile.

DOI: 10.31857/S00234761250112e2

INTRODUCTION

Quantitative characterization of non-uniform lattice strains in metals and alloys represents a fundamental objective in X-ray diffraction analysis [1]. Such studies are based on measuring the width of diffraction lines on X-ray patterns [2], they are complicated by the need to separate the instrumental broadenings associated with the final collimation of beams and the doublet nature of the radiation. Such separation is carried out by various mathematical methods using a reference undeformed sample carrying information about the instrumental function [3]. Such studies as a method of non-destructive testing have become increasingly relevant in connection with the widespread use of a new method of mechanical processing – deforming cutting (DC) [4–6].

The DC method allows obtaining macro-relief on various materials – steels and alloys based on titanium, copper, aluminum [7]. Macro-relief obtained by the DC method, in combination with various technological operations, is of significant interest for the creation of hardened surface structures with modified properties. The DC method is implemented on universal metal-cutting equipment with a tool with a special geometry of the cutting wedge. During DC, the cut layer is not removed in the form of chips, but is deformed, maintaining a single whole with the processed metal [4–6].

The creation of a vertical ribbed profile by the DC method on the surface of cylindrical parts is used to restore worn surfaces [6]. The DC method is considered promising for the creation of developed surface structures with increased wear resistance by carrying out chemical-thermal treatment of the pre-ribbed surface [7].

The presence of a regular macrorelief on a curved surface leads to additional broadening of diffraction lines, distorting data on the deformation of crystal lattices. It is important to separate these effects using mathematical processing of X-ray data.

The aim of this study is to develop a method for obtaining true intensity distribution profiles for identifying non-uniform surface deformations on a cylindrical surface using X-ray diffractometry supplemented by a mathematical method based on separating the effects associated with the influence of a curved surface with a regular sample relief on the shape of the diffraction profile. A mathematical data processing technique is used to obtain true intensity distribution profiles associated with non-uniform surface deformations and small block sizes. The technique is based on solving the problem of reconstructing the true line intensity distribution profile by solving integral equations using the regularization method of Academician A.N. Tikhonov [3, 8–10] while simultaneously eliminating other causes of additional line broadening associated with finite beam collimation and the doublet nature of the radiation.

METHODS AND MATERIALS

The samples of 08Kh18N10T steel according to GOST 5632-72 with the elemental composition: C – 0.08, Cr – 18, Ni – 10, Mn – 2, Si ⩽ 0.8, Ti ⩽ 0.6 wt. %, Fe – base were studied, on the curved (cylindrical) surface of which an inclined macrorelief was formed by the DC method (Fig. 1a-c).

Some of the samples were annealed in a vacuum furnace at 800°C for 2 hours to eliminate defects formed during DC. Three types of samples were used for X-ray studies: with a deformed ribbed surface, annealed samples with a pre-deformed ribbed surface, and an annealed sample with a flat surface. Samples with two types of ribbed macrostructure created by the DC method were studied, differing in the angle of inclination of the ribs to the axis of the cylindrical surface and the gap between the ribs (Fig. 1b, 1c).

To study non-uniform deformations in the surface layer of 08Kh18N10T steel at a cutting speed of 0.4 m/s and a cutting depth of 0.3 mm, an inclined macrorelief was formed with a step of 0.2 mm with different inter-rib gaps and inclination angles: DC-1 with an inter-rib gap of less than 0.02 mm at an inclination angle of about 50° and DC-2 with an inter-rib gap of 0.1 mm at an inclination angle of about 90° (Fig. 1b, 1c).

For samples after DC, the reflected beam from the surface profile with the studied deformation effect, starting from 70° for the angle 2θ, enters the detector area. For samples after DC-2 processing, the surface area of the deformation area is smaller than after DC-1 processing, and the studied deformed section has a different surface configuration of the deformation area (Fig. 1b, 1c). Rays for which reflection occurs only from the area marked in Fig. 1b, 1c can enter the detector. The contributions of deformations of crystal structures located near these surfaces at a depth of up to 7 μm are studied below.

X-ray studies were performed using an X'pert PANAnalytical diffractometer (CuK_α radiation, θ/2θ scanning mode in the angular range of 5°–140° with a step of 0.05° along the 2θ angle) with a curved monochromator installed between the sample and the detector. The effective penetration depth of CuK_α radiation in the studied alloy was 2–8 μm for this angle range. The obtained diffraction patterns were normalized to the total integrated intensity of the diffraction maxima. The phase composition was determined based on the ICCD PDF2 2019 and ICSD 2014 databases.

To obtain the true intensity distribution associated only with inhomogeneous deformations and the small size of the $fr(x)$ blocks, we used a method for separating instrumental broadenings and the $K_{\alpha 2}$ component of the K_α doublet, based on solving the Fredholm integral equation using the regularization method of A.N. Tikhonov [3]:

$$\int A(x, y)\, fr(x)dx = fexp(y). \qquad (1)$$

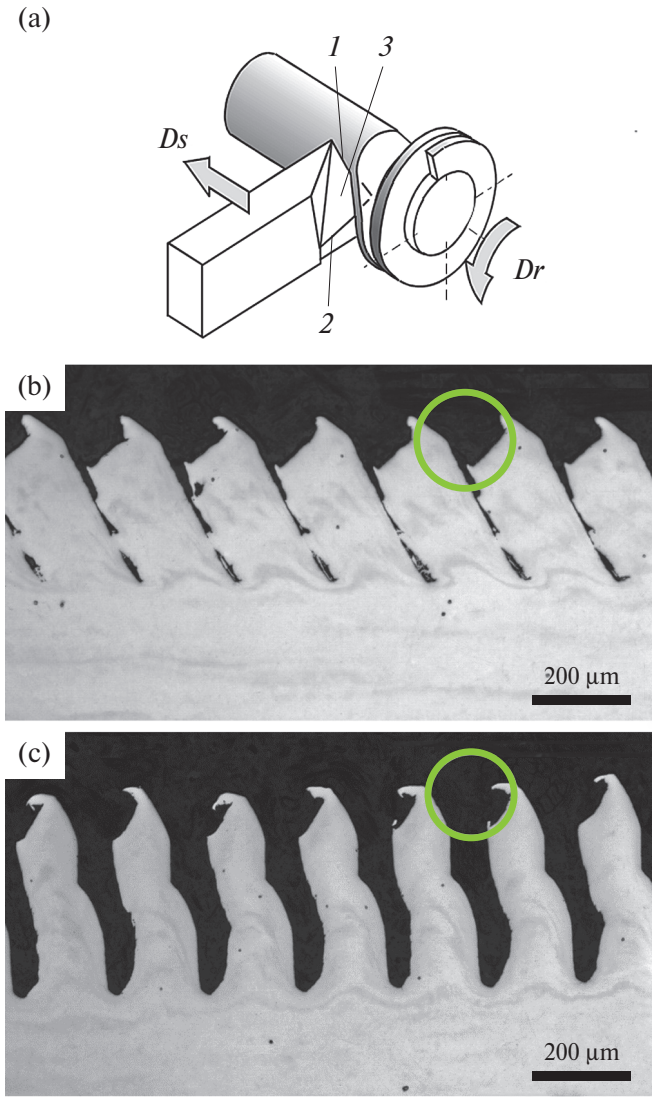

Fig. 1. Scheme of deforming cutting (a) and microstructure of the cross-section of ribbing on 08Kh18N10T steel after deforming cutting in DC-1 (b) and DC-2 (c) modes: *1* – main cutting edge, *2* – auxiliary (deforming) edge, *3* – front surface; *Dr* – main cutting movement; *Ds* – feed movement, the area examined by the X-ray method is marked with a circle.

In this case, the intensity distribution near the selected diffraction maximum of the sample after surface deformation, taking into account line broadening from all causes of broadening (inhomogeneous deformations, uneven sample surface, instrumental broadening and the effect of K_α-radiation doublet), was used as the experimental profile $fexp(y)$ (and the right-hand side of the Fredholm equation (1)) and a similar profile for the sample after the same surface deformation and annealing was used as the kernel $A(x,y)$ of the equation (for y, corresponding to the maximum of the profile intensity). According to [3], the kernel $A(x,y)$ of equation (1) is a set of functions

$A(x)$ of the intensity distribution over y, which yields (due to the effect of the uneven sample surface, finite collimation of the beams at angles and the doublet of the K_α-radiation) a perfect crystal with a single value of the interplanar distance and the associated diffraction angle y. The sought function $fr(y)$ is represented by its values at the nodes of a dense grid, the function $fexp(y)$ is represented as the sum of the functions $fr(x)$ over the grid nodes, multiplied by $A(x,y)$. In this case, even one grid node with the value $fr(y)$ will give contributions to the intensity at closely located nodes. The profile of the diffraction line of the sample after surface deformation and annealing was approximated by a K_α-doublet with the intensity distribution in the form of a Cauchy function:

$$f(x) = \frac{A}{\Gamma\left\{\left[\frac{x - x_c}{\Gamma}\right]^2 + 1\right\}^n} + \frac{A * R}{\Gamma\left\{\left[\frac{x - d - x_c}{\Gamma}\right]^2 + 1\right\}^n}, \quad (2)$$

$$d = \frac{\Delta\lambda}{\lambda}\operatorname{tg}(x / 2), \quad (2.1)$$

$$\Gamma = \Gamma_0 + \Gamma_1 x + \Gamma_2 x^2, \quad (2.2)$$

$$n = n_0 + n_1 x + n_2 x, \quad n \in [1.2;\ 1.9], \quad (2.3)$$

$$R = \frac{I(K_{\alpha 2})}{I(K_{\alpha 1})} = 0.508. \quad (2.4)$$

A is the normalization factor, $x = 2\theta$, x_c is the position of the maximum of the $K_{\alpha 1}$ line of the K_α doublet, the values Dl = 0.0038 and l = 1.5405 Å are taken from [3, 8, 9].

In this approach, we took into account the change in the type of the instrumental function with a change in the diffraction angle, namely the interdoublet distance d and the broadening of the lines Γ depending on the angle 2θ in the profile, depending on the selected parameters Γ_i, n_j. For this, first, for each profile of the (hkl) reflection of the sample after deformation and annealing, the values of R, Γ, A, x_c, n were selected using the least squares method. Then, the values of the parameters Γ_i, n_j of formulas (2.2) and (2.3) were selected based on the approximation of the values of the parameters n and Γ obtained for different reflections with different diffraction angles.

As a result of solving equation (1), we obtained the profile of the true intensity distribution $fr(x)$, by the shape of the line of which we determined the true line broadening, the nature and magnitude of inhomogeneous deformations and the sizes of crystalline grains.

The work also used a traditional method for assessing the contribution of the size of the coherent scattering region (**CSR**) and microdeformations to the reflection profile function – the Williams–Hall method [12–14] to control the separation of effects caused by DC.

DISCUSSION OF RESULTS

To obtain data on the true intensity distribution profile, Fredholm equations were solved using the diffraction line profile of a sample with a surface deformed by the DC method as *fexp* (1) and the instrumental function – the diffraction line profile of an annealed sample after the same deformation treatment (Fig. 2). It is evident that the true distribution profile (*4* in Fig. 2) is significantly narrower than the experimentally obtained one (*1* in Fig. 2) and is comparable in line width to the instrumental function profile, which confirms the significant contribution of instrumental broadening, doublet K_α radiation and sample surface roughness to line broadening in this case.

The result of solving the Fredholm equation (*4* in Fig. 2) shows the blurring of the profile only under the influence of "physical causes" – non-uniform deformations and grain sizes.

Thus, the line broadenings from *1* – deformations, *2* – the curved surface of the sample, *3* – instrumental broadenings and the influence of the K_α-doublet are comparable, and in this case the instrumental functions can be described by the Cauchy function (2).

The true intensity distributions for reflections 220, 311, 222 were obtained (Figs. 2–4). These distributions carry information about non-uniform deformations along the scattering vector (coinciding with the normal to the sample surface in this case) for interplanar distances d_{220}, d_{311}, d_{222}.

Separation of the instrumental function and the contribution from the curved surface obtained by the DC method to the profile of the diffraction lines of

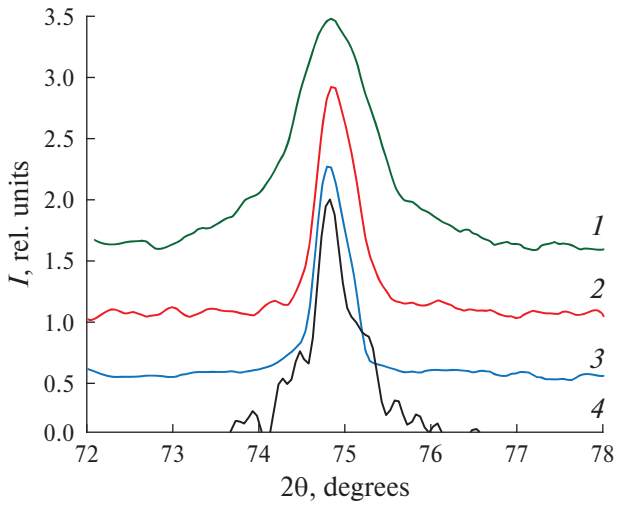

Fig. 2. Distribution of intensity in the 220 reflection profile for samples after: *1* – ribbing, *2* – ribbing and annealing, *3* – annealing without ribbing; *4* – result of solving the Fredholm equation, corresponding to the blurring of diffraction maxima, only due to inhomogeneous deformations and grain size.

the sample after DC made it possible to obtain the true distribution of the profile intensity. Based on the obtained true intensity values, the profile parameters and true values of the lattice parameters of the phase – a solid solution based on face-centered iron – were calculated: using the wavelength of the $K_{\alpha 1}$ component for the true profile of 3.5910 Å and the weighted wavelength of the $K_{\alpha 1,2}$ components for the original ribbed sample – 3.5884 Å, for the ribbed annealed – 3.5854 Å, for the flat annealed – 3.5902 Å.

The blurring of the true intensity distribution profile turns out to be asymmetric with characteristic maxima shifted relative to the $K_{\alpha 1}$ maximum of the profile (*4*) of the flat annealed sample (Fig. 3). The intensity distributions corresponding to reflections 311, 220 and 222 substantiate the distribution of deformations in the corresponding directions based on the measurement of the distribution of interplanar distances d_{220}, d_{311}, d_{222}. Four maxima are observed in the distribution for 311, two maxima at smaller angles correspond to increased d_{311} in the direction of the scattering vector (in this case perpendicular to the sample surface), two maxima at larger angles correspond to decreased d_{311}. With the second changed cutting mode, these four maxima are preserved, the relative height of the third maximum, corresponding to small compressive deformations, decreases (*1* and *2* in Fig. 4).

For the d_{222} distribution, three maxima are observed: the first, the strongest, corresponds to stretched d_{222}, the second strong one corresponds to slightly changed d_{222}, and the third one corresponds to compressed sections for which d_{222} is reduced. For the second DC mode, an additional maximum appears at small angles, corresponding to strong stretches (*1* and *2* in Fig. 4). Similar maxima are observed for the d_{220} distribution (Table 1).

For each considered intensity distribution, the microdeformations and block sizes were estimated using the Debye–Scherrer and Williams–Hall methods without preliminary mathematical processing. The obtained values of microdeformations and block sizes are given in Table 1.

The data obtained in the work made it possible to determine the parameters of the maxima of the true intensity distributions (*4* in Fig. 2 and *1* in Fig. 4) and the corresponding values of d_{hkl}, relative deformations $d_{hkl}/\langle d_{hkl}\rangle$ and the spread of $d_{hkl}/\langle d_{hkl}\rangle$ (Table 2).

When comparing the microdeformations given in Tables 1 and 2, it is easy to notice the correlation between the microdeformation values obtained by classical methods and the method proposed in this paper. However, classical methods do not allow one to construct the d_{hkl} distribution function and distinguish differently deformed regions for a separate d_{hkl}, which does not allow one to judge the nature and type of deformation.

The results of calculating the parameters of microdeformations obtained for the profiles of true

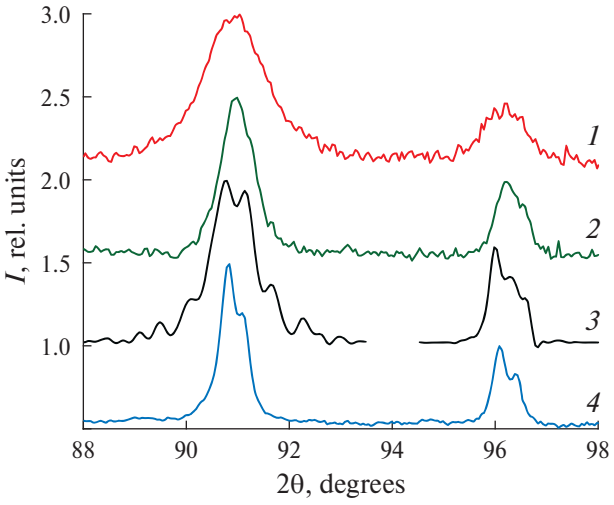

Fig. 3. Distribution of intensity in the reflection profile 311 and 222 for samples: *1* – after ribbing by the DC-1 method, *2* – annealing with a treated surface by the DC-1 method, *4* – a sample with a flat surface; *3* – the result of solving the Fredholm equation, corresponding to the blurring of diffraction maxima only due to inhomogeneous deformations of the DC-1.

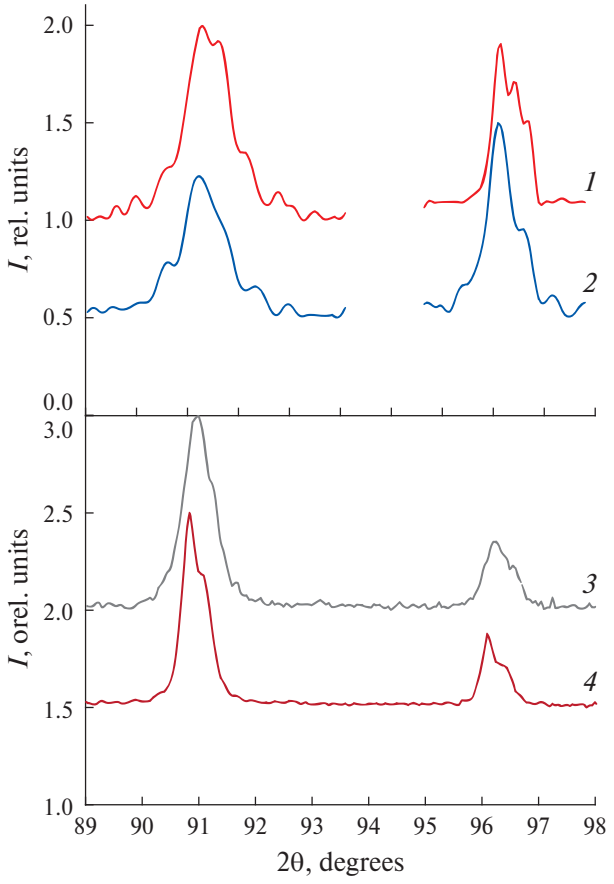

Fig. 4. Comparison of the reflection profiles (311) and (222) of annealed samples with different interfin gaps after DC-1 and DC-2 of samples (*3* and *4*); true reflection profiles (*1* and *2*) for samples not annealed after the DC, corresponding to graphs *3* and *4*. Graphs *1* and *2* are given with an increased intensity scale.

intensity distributions (Table 2) are associated with several maxima in the distribution of interplanar distances d_{220}, d_{311}, d_{222}. From the data obtained it follows that in the sample for one reflection there are several differently deformed regions, forming a superposition of contributions to the distribution of microdeformations and the shape of the diffraction maximum.

To obtain data only on the effect of sample surface roughness on line broadening and shape, the Fredholm equation was solved using the diffraction line profile of an annealed sample with a pre-deformed ribbed surface (*3*, *4* in Fig. 4) as *fexp*, and with a flat surface after annealing (*4* in Fig. 3) as the instrumental function. The results of solving equation (1) are presented for two DC variants (Fig. 5).

As a first approximation, the curves shown in Fig. 5 can be approximated by Cauchy functions given by formula (2) for one maximum.

When comparing the profiles of samples with different inter-rib gaps in Fig. 1b, 1c after separating the

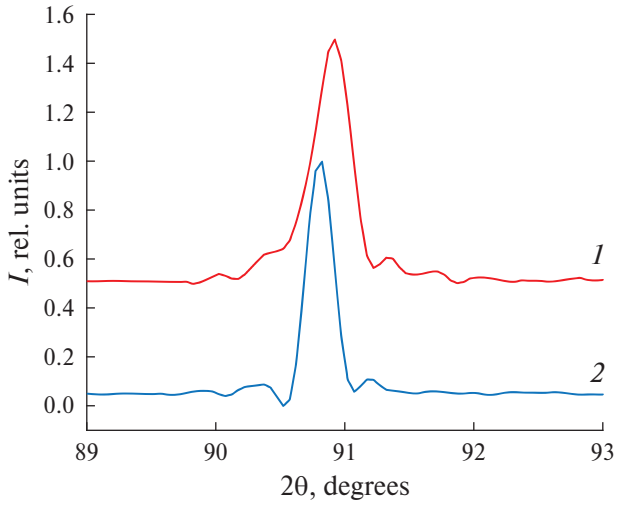

Fig. 5. Intensity distribution characterizing only the contribution from the curved surface for the profiles shown in Fig. 4 (*3* and *4*): *1* – profile of sample DC-1, *2* – profile of sample DC-2.

Table 1. True values of crystal lattice microdeformations obtained as a result of data processing for the DC-2 case using classical methods, obtained from profiles *1* shown in Figs. 2, 4

hkl	$2\theta_{max}$, deg	d_{hkl}, Å	Debye-Scherrer		Williams–Hall	
			ε, %	CSR, Å	ε, %	CSR, Å
220	74.685	1.2699	0.0436	441	0.1607	394
311	90.508	1.0845	0.0806	550	0.1525	352
222	95.853	1.0377	0.0744	905	0.1149	450
			0.0662	632	0.1427	399

Table 2. Parameters of the maxima of the true intensity distributions *4* in Figs. 2, 4 and the corresponding values of d_{hkl}, relative deformations $d_{hkl}/\langle d_{hkl}\rangle$, and the spread of $d_{hkl}/\langle d_{hkl}\rangle$

hkl	$2\theta_{max}$, deg	d_{hkl}, Å	*I*	$\langle d_{hkl}\rangle$, Å	$(d_{hkl} - \langle d_{hkl}\rangle) / \langle d_{hkl}\rangle$ %
220	74.1884	1.2772	19.3	1.2683	0.702
	74.6852	1.2700	48.2		0.129
	75.1295	1.2635	32.5		–0.377*
311	89.8371	1.0909	20.7	1.0818	0.844
	90.5080	1.0846	27.5		0.257
	90.9982	1.0800	20.6		–0.165*
	91.4851	1.0755	31.1		–0.580*
222	95.8539	1.0377	62.2	1.0358	0.187
	96.1268	1.0355	21.3		–0.027*
	96.1466	1.0354	16.4		–0.042*

Note. *The "–" sign indicates the "compression" area.

instrumental function in Fig. 4, one can see differences in the splitting of the profiles depending on the size of the inter-rib gap and the angle of inclination of the ribs. This effect is especially evident at large angles for reflections 311, 222, as expected, since for large angles the possibility of rays scattered by large (and deep) areas of the surface entering the detector is ensured.

As can be seen in Fig. 5, the width of profile *1* is noticeably greater than the width of profile *2*, the center of gravity of the profile in the case of DC-1 is shifted to larger angles compared to DC-2, this is due to the change in the area of the ribbing profile of the sample, from which the reflection of the primary beam occurs (Fig. 1b, 1c).

CONCLUSION

A technique for obtaining true diffraction intensity distribution profiles has been developed, which allows determining non-uniform deformations of surface layers using the X-ray diffractometry method and separating the effects associated with the influence of a curved surface and regular sample relief on the shape of the diffraction profile using mathematical methods. The contribution from the $K_{\alpha 2}$ doublet and instrumental broadenings is also separated, and changes in these contributions are taken into account when the diffraction angle changes. When implementing mathematical processing, a solution was used to the problem of restoring the true line intensity distribution profile using the solution of the integral equation using the regularization method of Academician A.N. Tikhonov [3, 12], taking into account in the instrumental functions (1) the causes causing additional line broadenings associated with the influence of a curved surface and regular sample relief, as well as the final collimation of the beams and the doublet nature of the radiation.

True intensity distribution profiles associated with non-uniform surface deformations and sizes of coherent scattering blocks that arose during deformation cutting on a fundamentally uneven surface with a regular relief of a 08Kh18N10T steel sample were obtained.

The features of the distribution functions of non-uniform deformations of surface layers that arose along the directions 220, 311 and 220 during deformation cutting on the surface of a sample of 08Kh18N10T steel after two modes of deformation cutting were revealed. These functions have three to four characteristic maxima corresponding to compressions and tensions of the crystal lattice along these directions; the shape of the maxima depends on the reflection indices and the mode of deformation cutting. The blurring of the profile of the true intensity distribution turns out to be asymmetric with the characteristic maxima shifted from the original sample relative to the profile (*4* in Fig. 3). The intensity distribution from the change in interplanar distances substantiates the distribution of deformations along the corresponding directions corresponding to reflections 311, 220 and 222.

A comparison of the two DC methods showed that there is a noticeably greater splitting of the profiles (*1*, *2* in Fig. 4) of reflections 311 and 222 in DC-2 with a surface that has a more complex relief with a large difference in the depth of areas capable of contributing to X-ray diffraction.

Analysis of the true profiles of individual diffraction maxima allows us to determine the distribution functions of crystallite deformations in different directions, the features of the deformed state of crystallites in the surface region of the sample caused by deformation treatment, and to predict the prospects for subsequent chemical-thermal treatments of these materials.

FUNDING

No additional grants to carry out or direct this particular research were obtained.

ETHICS DECLARATION

This work does not contain any studies involving human and animal subjects.

CONFLICT OF INTERESTS

The authors of this work declare that they have no conflicts of interest.

REFERENCES

1. *Aero E.L.* // Vestn. of the Perm technical un-ty. Mechanics. 2006. No. 14. P. 27.
2. *Krivoglaz A.M.* Diffraction of X-rays and neutrons in non-ideal crystals. Kyiv: Naukova Dumka, 1983. P. 407.
3. *Vintaikin B.E. and Kuzmin R.N.* // Kristallografiya. 1986. V. 31. No. 4. P. 656.
4. *Zubkov N.N., Ovchinnikov A.I.* Method for producing surfaces with alternating protrusions and depressions (variants) and a tool for its implementation: patent 2044606 RF // Bulletin No. 27. 1995.
5. *Neustroev V.S., Markelov D.E., Obukhov A.V. et al.* // Materials Science Issues. 2021. V. 4. No. 4 (108). P. 233.
6. *Zubkov N.N.* // Repair, restoration, modernization. 2003. V. 10. P. 7.
7. *Zubkov N.N., Ovchinnikov A.I., Vasiliev S.G.* Method of hardening the surface of a part: patent RU 2 015 202 C1. 1994.
8. *Vintaikin B.E., Smirnov A.E., Cherenkov Y.V.*// Crystallogr. Rep. 2022. V. 67. P. 602. https://doi.org/10.1134/S1063774522040186
9. *Vintaikin B.E., Kamynin A.V., Kraposhin V.S. et al.* // J. Phys: Conf. Ser. 2017. No. 918. P. 012014. https://doi.org/10.108/1742-6596/918/1/012014

10. *Guinier A*. X-ray diffraction of crystals. Moscow: Phys.-Math. Literature, 1961. P. 604.
11. *Langford J.L., Prince E., Stalick J.* // Mater. Sci. Eng. Lab. 1992. V. 2. P. 110.
12. *Halder N.C., Wagner C.N.J.* // Acta Cryst. 1966. No. 20. P. 312.
13. *Williamson G.K., Hall W.* // Acta Metallurgica. 1953. No. 1. P. 22.
14. *Aleksandrova N.M., Cheretaeva A.O., Mishet'yan A.R. et al* // Met Sci Heat Treat. 2021. V. 62. P. 669 https://doi.org/10.1007/s11041-021-00621-9